Structure-astringency relationship of anacardic acids from cashew apple (*Anacardium occidentale* L.)

Liana Maria Ramos Mendes[a,b], Deborah dos Santos Garruti[b], Guilherme Julião Zocolo[b], Marcelo de Freitas Lima[c], Edy Sousa de Brito[b,*]

[a] Departamento de Engenharia Química, Universidade Federal do Ceará, Fortaleza, Brazil.

[b] Embrapa Agroindústria Tropical, Rua Dra Sara Mesquita, 2270, Pici, Fortaleza, CE, 60511-110, Brazil

[c] Universidade Estadual Paulista (Unesp), Instituto de Biociências Letras e Ciências Exatas, Departamento de Química e Ciências Ambientais, São José do Rio Preto, SP, 15054-000, Brazil

[*]Corresponding author: Edy Sousa de Brito

E-mail addresses: mendes_liana@hotmail.com (L.M.R. Mendes), deborah.garruti@embrapa.br (D.S. Garruti), guilherme.zocolo@embrapa.br (G.J. Zocolo), marcelo.f.lima@unesp.br (M.F. Lima), edy.brito@embrapa.br (E.S. de Brito)

ABSTRACT

Cashew apple presents a characteristic astringency. However, the compounds responsible for this characteristic were not described yet. A cashew apple extract was added to a BSA solution and the compounds before and after precipitation were analyzed by UPLC-QTOF/MS^E. The extract astringency was measured on a 5-point scale (0: non astringent and 4: extremely astringent). Among the phenolics detected anacardic acids were identified and evaluated for their astringent effect. In the sensorial tests the cashew apple extract was considered very astringent (average of 2.5). A mixture of anacardic acids, had an average of 1.76 (astringent). The three isolated anacardic acids were evaluated. The *in silico* experiments were performed to analyze mainly the steric factor associated to the binding. The sensory results were confirmed by *in silico* analysis, indicating that a higher unsaturation degree of the aliphatic chain leads to an astringency increase.

Keywords: anacardic acid; astringency; cashew apple; docking; ginkgolic acid; *in silico*.

1. Introduction

The cashew apple is a peduncle which supports the cashew nut. It can be consumed *in natura*, but also has good characteristics for processing due to its juicy pulp, high sugar and vitamin C content; and flavor. Despite its nutritional and functional potential, the cashew apple still presents low consumption when compared to other fruits, mainly due to its astringency.[1]

Astringency is defined as a set of wrinkling sensations of the oral epithelium after exposure to substances such as aluminum or tannins. This sensation can be perceived by consumers as a "puckered" taste and throat irritation. Despite the importance of astringency for some products, the mechanisms of this attribute are not well known, so it is necessary to deepen the methodologies of astringency study.[2] The most accepted mechanism to explain how astringency occurs was proposed by Siebert, Carrasco, & Lynn, 1996,[3] in which the protein has a fixed number of sites to which the tannins can bind, while each polyphenol also has its fixed number of bonds. When the total number of polyphenol and protein bonds are the same, the largest complex and maximum precipitation will be produced.[2]

New sensory and analytical techniques have been developed and used together in an effective procedure for the screening of non-volatile compounds important for the taste of food. This approach, combining instrumental analysis and human response led to the discovery of several previously unknown compounds such as the bitter and astringent compounds of different products.[4–6] To solve the problem of astringency, it is necessary to identify the compounds present in the cashew apple that are responsible for this characteristic and, thus, to develop methodologies, extraction systems or even genetic modifications in cashew clones, aiming to decrease or eliminate the astringent compounds. The objective of this work was to identify the cashew apple components responsible for its astringency using sensory, instrumental and computational analysis.

2. Material and Methods

2.1. Reagents

The reagents used were methanol HPLC (purity ≥ 99.9%, LiChrosolv®, Germany); acetonitrile HPLC (purity ≥ 99,9%, Tedia, Fairfield, OH, USA); glacial acetic acid P.A. (purity ≥ 99,7%); genistein and methanol P.A. (purity ≥99,8%), purchased from Sigma-Aldrich (Saint Louis, MO, USA); and purified water from an Mili-Q system (Millipore, São Paulo, Brazil).

2.2. Cashew Apples

Cashew apples from clone CCP 09 were used for the compounds extraction. The fruits were harvested on the Embrapa experimental field located at Pacajus-CE, Brazil (4°11'26,62" S; 38°29'50,78" W), harvested in 2017 (September to November). After being sanitized the peduncles were freeze-dried and grinded. The samples were packed under vacuum and stored at -20º C until further use.

2.3. Extraction of cashew apple phenolics

Freeze-dried cashew apples (50 g) were extracted with methanol-water 60:40 (v/v) in an ultrasonic bath (Ultrasonic Cleaner 1400, Thornton/UNIQUE, São Paulo, Brazil), at 40 kHz, 100W, temperature of 25º C for 30 min. The mass:volume ratio used was 1:10 (m/v), being the extraction performed with ten replicates. Subsequently, the samples were centrifuged at 2,944 *g* for 15 min and the supernatants combined. The extract was dried under reduced pressure at 40° C, followed by freeze-drying to assure methanol removal.

2.4. Protein Precipitation

Protein precipitation was performed on the methanolic extract of the cashew apple with bovine serum albumin (BSA), according to the methodology described by Hagerman & Butler, 1978,[7] with adjustments. To 1.0 mL aqueous solution of the cashew apple extract was added 2.0 mL of BSA solution (1.0 $mg.mL^{-1}$) in a 15 mL centrifuge tube. After vortexing for 1 min, it was allowed to stand 24 h at 8 ^{o}C for precipitation. After precipitation, the complex was centrifuged (2,944 *g* for 15 min) obtaining the supernatant (non-complexed phenolics) and the precipitate.

The precipitate was gently washed with water, centrifuged (2,944 *g* for 10 min) and the precipitate was extracted with methanol on an ultrasound bath (5 min) and centrifuged. The extraction process was repeated four times and the combined methanolic extract was dried under reduced pressure at 40° C and freeze-dried (cashew-protein precipitate extract).

To obtain sufficient phenolics for sensory analysis, the above protein precipitation process was carried out on a larger scale, respecting the proportions of methanolic extract and protein, only that BSA was substituted by an aqueous solution of commercial gelatin.

2.5. UPLC-QTOF-MS^{E} profile

The analysis was performed using an Acquity UPLC (Waters, Milford, MA, USA) system, coupled with a Quadrupole/TOF (Waters) system.[8] A Waters Acquity UPLC BEH column (150 × 2.1 mm, 1.7 μm) was used, with the column temperature set at 40 °C. The binary gradient elution system consisted of 0.1% formic acid in water (A) and 0.1% formic acid in acetonitrile (B). The UPLC elution conditions were optimized as follows: linear gradient from 2% to 95% B (0-15 min), 100% B (15-17 min), 2% B (17.01), 2% (17.02-19.01 min), a flow of 0.4 $mL.min^{-1}$, and a sample injection volume of 5 μL. The chemical profiles of the samples were determined by coupling the Waters ACQUITY UPLC system to a QTOF mass spectrometer (Waters) with the electrospray ionization interface (ESI) in negative ionization mode. The ESI^{-} mode was acquired in the range of 110–1180 Da, with a fixed source temperature of 120 °C and a desolvation temperature of 350 °C. A desolvation gas flow of 500 L.h^{-1} was used for the ESI^{-} mode. The capillary voltage was 2.6 kV. Leucine enkephalin was used as a lock mass. The MS mode used Xevo G2-XS QToF. The spectrometer operated with MS^{E} centroid programming using a tension ramp from 20 to 40 V. The instrument was controlled by the MassLynx 4.1 software program (Waters Corporation, USA). The samples were spiked with genistein (1ppm) internal standard.

2.6. Fractionation of anacardic acids

Anacardic acids were obtained by preparative HPLC fractionation of cashew nut shell liquid (CNSL) as described by Oiram Filho, Zocolo, Canuto, Silva Junior, and de Brito, 2019.[9] The compounds present in the anacardic acid mixture were isolated on a reverse phase chromatographic column Waters SunFirePrep C18 OBD (100 x 19 mm x 5 μm). The mobile phase was used in an isocratic mode using methanol, water and acetic acid in the proportion (90:10:1), run time of 40 min, and a flow of 3 mL.min^{-1}, at 25 ºC. The injection volume was of 1 mL at a concentration of 100 mg.mL^{-1}. The chromatograms were monitored at a wavelength of 280 nm.

The yield obtained for the triene, diene and monoene anacardic acids were 22.1, 13.3 and 17.5 %, respectively. The purity of each anacardic acid isolated was monitored by HPLC[10] and the values were 98.93 %, 72.67 % and 79.68 % for triene, diene and monoene, respectively. The purity values of the compounds were satisfactory since, in the literature, studies reported isolation of phenolic compounds from purities between 75 and 99%. [11]

2.7. Sensory Analysis

The sensorial test was performed by previously selected and trained panelists, using test protocols approved by a Research Ethics Committee under Opinion n° 147.279. Before the tests were run, the panelists were asked to sign a Free and Informed Consent Form (TCLE).

The analyzed samples were: methanolic cashew extract (ME), cashew protein precipitate extract (PPE), anacardic acid mixture (AnMix) and anacardic acids (An1, An2, An3). The samples were solubilized in bottled water with ºBrix and pH adjusted for the mean values of *in natura* cashews (7.1 and 4.15, respectively). The concentrations were defined according to the phenolic concentration values found in the literature for the cashew apple, in the range of 1 to 2 $mg.mL^{-1}$.[12] All samples were analyzed with repetition and the minimum interval between sessions was 10 min.

The concentrations for sensory analysis were 2 and 5 $mg.mL^{-1}$ for the methanolic cashew extract (ME2 and ME5 respectively); 1 and 2 $mg.mL^{-1}$ for the cashew protein precipitate extract (PPE1 and PPE2 respectively); 1 $mg.mL^{-1}$ for anacardic acid mixture (AnMix), anacardic acid 15:1 (An1), anacardic acid 15:2 (An2); and anacardic acid 15:3 (An3).

Five mL of samples were served in 50 mL cups in a monadic sequence. The panelists were asked to put all the container contents in the mouth and let it stand for 10 s, roll the solution through the mouth, exposing it to all taste buds and buccal mucosa (at least 3 rotations) and then spit the solution into a container. After 15 s, the panelists marked the perceived astringency intensity on a 5-point scale (0 = not astringent, 1 = little astringent, 2= astringent, 3 = very astringent; and 4 = extremely astringent). The minimum and maximum extremes of the scale were previously determined in training.

2.8. Statistical Analyses

The results obtained in the sensorial astringency tests were submitted to analysis of variance (ANOVA) with the following sources of variation: sample (SAMP), assessor (ASSE) and the interaction SAMP X ASSE, being the assessor considered as a block. Significant differences between means were determined by the Ryan-Einot-Gabriel-Welschand Quiot test (REGWQ) with confidence interval of 95% ($\alpha = 0.05$). The analyses were performed using the statistical program XLSTAT v. 18.1 (Addinsoft).

2.9. Computational method

The structures of the three anacardic acids (ene-derivatives of the salicylic acid) were built and optimized using Avogadro (version 1.0.3) using MMFF94 force field [13] and all of them based on the benzoic acid residue found in the active site of 6DHB. [14] Topology of the ligands for MD simulation were generated via the CGenFFserver. [15] As the penalty scores from CGenFF were lower than 50, no further optimization was taking in account. All MD simulations were carried out using the GROMACS software package (version 5.0.2). [16]

An initial model of each protein-ligand complex in dodecahedral box filled by TIP3P water was constructed using the editconf and solvate tools of GROMACS. Z-

Length of simulation box was determined by water thickness, minimum water height on top and bottom of the system was set to 10 Å. The net charge on the system was neutralized by adding Na^+ ions. The charmm36 force field [15,17–20] was used for all systems and simulations. The system was gradually relaxed according to position and angle restraint conditions to reach equilibrium (300 K, 1 atm). Then, 10 ns NPT (constant number of atoms, pressure, and temperature) simulation without any position restraint with 2 fs time step was performed. In NPT simulation, temperature and pressure were regulated using the V-rescale thermostat algorithm [21] and the Berendsen barostat algorithm, [22] respectively. The time constant for the temperature and pressure coupling was kept at 0.1 and 2.0 ps, respectively. The pressure was coupled with isotropic scheme with isothermal compressibility of 4.5×10^{-5} bar^{-1}. The short-range nonbonded interactions were computed for the atom pairs within the cutoff of 1.2 nm, while the long-range electrostatic interactions were calculated using particle-mesh-Ewald summation method with fourth-order cubic interpolation and 0.16 nm grid spacing. The same method was reproduced for all simulations. All PDB files of the ligands are transcripted in the Supporting Information section. The files of the protein and protein-ligand complexes are provided in the same section as PDB files.

3. Results and Discussion

Table 1 shows the compounds that were tentatively identified in cashew extracts samples based on their fragment ions as well as a comparison with data from the literature. Among the identified compounds, pentagaloyl hexoside, a precursor for the formation of more complex ellagitannins and gallotannins was present in all samples analyzed. Three ancardic acids with C15 alkyl chain length and different degrees of unsaturation (tri, di and mono-unsaturated) were identified in the extracts, and one anacardic acid with C17 alkyl chain was present in the methanolic extract of the cashew apple and in the cashew protein precipitate extract. Anacardic acids are phenolic compounds derived from salicylic acid, and due to their aliphatic chain, have lipid characteristics. [23] They are present in higher concentration in the cashew nut shell liquid.[10] In cashew apple the concentration of these compounds varies from 0.20 to 0.51 %.[24] As shown in Table 1, the phenolics that precipitate alongside the protein had the same profile as the cashew methanolic extract. However, the anacardic acid 1 7:1 was not detected on the protein non-complexed fraction, probably due to its low concentration.

The combination of sensory analysis with analytical techniques (bioguided isolation) has been of great importance for the recognition of several compounds that influence the sensorial characteristics of food products. In order to identify the chemical markers for astringency in the cashew apple, the astringency test was performed with the samples mentioned in the previous sections. Due to the presence of anacardic acids in the protein precipitate extract, a sensory analysis of a mixture of major anacardic acids (approximately 50 % for An3, 20 % for An2 and 30 % for An1), as well as the isolated compounds, was performed. A significant difference was observed among the samples regarding the intensity of astringency perceived by the sensory panelists. The means were compared by means of the REGWQ test; whose results are shown in Fig.1.

Cashew apple methanolic extracts at concentrations of 2 and 5 $mg.mL^{-1}$ presented low astringency, scoring below 1.0, between ‘not astringent’ and ‘little astringent’ in the 5-point scale. The cashew protein precipitate extract in the concentration of 1 $mg.mL^{-1}$ scored 1.12 (‘little astringent’), however, when its concentration was doubled, the astringency perception increased, reaching 2.50 points, considered between “astringent” and “very astringent” by the panelists. Those results make clear that the protein precipitation was selective to concentrate the astringent compounds in the extract, since the sensory astringency perceived in cashew protein precipitate extract is statistically greater than in methanolic cashew extract.

The anacardic acid mixture (concentration of 1 $mg.mL^{-1}$) showed an intermediate astringency (1.75) between the two protein precipitate extracts, but not differing statistically from cashew protein precipitate extracts (1 and 2 $mg.mL^{-1}$). Although the sensory panel was trained with reference samples for astringency intensity, the individuals reported a difficult to classify the samples as very or extremely astringent, probably because they were accustomed to the high astringency of cashew apples. This fact may lead the use of a shorter interval on the scale, with a maximum of 4 points, thus reducing the sensitivity of the test in detecting significant differences among the samples.

For this same reason, there was also no difference between the anacardic acid mixture and the isolated anacardic acids. The triene anacardic acid (C15:3) reached 2.01 points (“astringent”), diene anacardic acid (C15:2) scored 1.63, and monoene anacardic acid (C15:1) averaged 0.86 (“little astringent”). However, monoene and triene anacardic acids differed statistically from each other. The panelists described a sensation of stinging followed by throat irritation after tasting the anacardic acids. The throat irritation and roughness in the mouth, named astringency subqualities, are common in the perception of astringency in the human palate and are even perceived after ingestion of cashew juice.

In lack of a specific protein or receptor responsible for the astringency sensation and in the attempt to justify the stronger interaction of the anacardic acid triene we have used the T-cell immunoglobulin and mucin-domain containing-3 crystallized with a benzoic acid residue (6DHB). As this protein have great affinity for derivatives of the salicylic acid, [14] we have conducted the *in silico* experiments to analyze mainly the steric and electrostatic factors associated to the energy of binding (Table 2). The decomposition of the short-range energies, from Coulombic and Lennard-Jones models, shows the major stability of the triene in comparison to the mono and the diene.

The total interaction energy, Coulombic plus Lennard-Jones (and propagating the error according to the standard formula for addition of two quantities) for the triene (C15:3) gives a total value of -155.3892 ± 8.5 kJ mol^{-1}, lower than -117.3290±25.2 kJ mol^{-1} and -146.5156±13.1, for mono and diene, respectively, confirming the indicatives shown by the decomposed parts. In a complementary way, we have analyzed the values of RMSD (data not shown), calculated from the protein backbone to the structure of the ligand. The data show how much the ligand binding pose has changed over the course of the simulation, adding more information regarding the more instable nature of the complex involving the monoene, which indeed make sense, considering the higher translational freedom degree of the hydrocarbon tail, compared to the more rigid triene.

Fig. 2 shows information for the 10 ns simulation concerning the three anacardic acids. First of all, we can point the instability of the protein-ligand complex involving the monoene (Fig. 2a), once it departs from the active site after about 5 ns of simulation. The di and triene, although stays attached, we, could see a lesser interaction between the side chain of the triene, more rigid, compared to the diene, following the energetic parameters presented in Table 2.

For an even more detailed look at how the ligands are interacting with 6DHB, we have computed the distance between the carboxyl and hydroxyl groups of anacardic acids and the amino group of three very important aminoacids of the active site of 6DHB

(Fig. 3). Exactly as reported by Golebiowski, Fiorucci, Adrian-Scotto, Fernandez-Carmona, & Antonczak, 2011, [25] studying the astringency of tannins, the main nature of the binding process of the astringency lies on the formation of hydrogen bonds, and for that, the backbone of the protein is more important than its side-chains. Another characteristic, also corroborated by Cala et al., 2012[26] is that the ligand (in their case tannins) has preferentially been found in the hydrophilic site of some proteins segments responsible for the astringency response. We have considered here that a hydrogen bond is formed when the donor and the acceptor are at most 3.5 Å apart (≤ 0.35 nm). As shown in Table 3, the stronger hydrogen bond is formed from the triene to the aspartate residue (residue 98 from 6DHB), all values indicate the more favorable formation of hydrogen bonds between the triene and 6DHB. As highlighted by Fig. 3, we can clear see that the hydroxyl group has more stereo advantage regarding the hydrogen bond to 6DHB than the carboxyl group.

Docking studies of anacardic acid and different proteins have been performed. For the matrix metalloproteinases, MMP-2/gelatinase A and MMP-9/gelatinase B, placed the head group in the aliphatic pocket, with the carboxylate group functioning as a zinc-binding group and forming a hydrogen bond to the active site of MMP-2; and the hydroxyl group of anacardic acid also forms a hydrogen bond to backbone oxygen of Ala192. [27] The anacardic acid carboxylate group also functions as a zinc-binding group in MMP-9 and forms a hydrogen bond to the Glu402 side chain, while the hydroxyl group of anacardic acid forms a hydrogen bond to backbone oxygen of Ala189. With parasitic sirtuins was observed the pose of anacardic acid in the TcSIR2rp1 pocket forming hydrogen bonds between the carboxylic group of the ligand and the side chain of Arg50.[28] Regarding the estrogen receptor α (ERα)–expressing breast cancer cell lines it was proposed that the alkyl chain of anacardic acid may be an important factor, in combination with the salicylic moiety, for high affinity for the ERα DBD and no affinity for the ERα LBD.[29] Anacardic acid interaction with the steroid receptor coactivator (Src)/focal adhesion kinase (FAK) was evaluated and mechanistically, it was proposed that it could dock into the hydrophobic pocket of Src and FAK protein.[30] The anacardic acid interaction with SIRT isoforms, which are class III histone deacetylases (HDACs) also revealed that it made hydrogen bonds, through its carboxyl group and hydroxyl group. It also verified that the rigidification of the tail could promote stable hydrophobic interactions with the pockets, decreasing the flexibility, and therefore the entropy of the systems.[31]

In conclusion, the astringent effect of anacardic acids was observed and described for the first time. The protein precipitation method revealed a profile similar to the extract, especially phenolics in the protein precipitate as revealed by UPLC-ES-QTOF-MS^E. The isolation of anacardic acids allowed the sensory evaluation and the ranking of astringency of these compounds was established based on the unsaturation pattern. Apparently, a higher unsaturation degree of the anacardic acid aliphatic chain leads to an increase on astringency. The triene was more astringent when compared to the monoene. The sensory data was corroborated by *in silico* analysis of the interaction energy of anacardic acids and a mucin, which demonstrated a stronger interaction of triene as compared to monoene anacardic acids.

authorship contribution statement

Liana Mendes: Conceptualization, Methodology, Validation, Investigation, Writing - original draft, Writing - review & editing. **Deborah dos Santos Garruti:**

Conceptualization, Methodology, Investigation, Writing - original draft. **Guilherme Julião Zocolo:** Methodology, Writing - original draft. **Marcelo Freitas Lima:** Methodology, Investigation, Resources, Writing - original draft, Writing - review & editing. **Edy Sousa de Brito:** Conceptualization, Methodology, Validation, Investigation, Resources, Writing - original draft, Writing - review & editing, Supervision.

Declaration of Competing Interest

The authors declare that they have no known competing financial interests or personal relationships that could have appeared to influence the work reported in this paper.

Acknowledgments

The Embrapa is acknowledged for financial support (13.16.04.006). LMRM acknowledge the scholarship by FUNCAP.

References

(1) Talasila, U.; Vechalapu, R. R.; Shaik, K. B. Clarification , Preservation , and Shelf Life Evaluation of Cashew Apple Juice. **2012**, *21* (3), 709–714. https://doi.org/10.1007/s10068-012-0092-3.

(2) García-estévez, I.; Escribano-bailón, M. T. Function and Human Saliva in Astringency Perception. **2018**, No. 2004, 1294–1309. https://doi.org/10.1039/c7fo02030a.

(3) Siebert, K. J.; Carrasco, A.; Lynn, P. Y. Formation of Protein-Polyphenol Haze in Beverages. *J. Agric. Food Chem.* **1996**, *44* (8), 1997–2005. https://doi.org/10.1021/jf950716r.

(4) Czepa, A.; Hofmann, T. Structural and Sensory Characterization of Compounds Contributing to the Bitter Off-Taste of Carrots (Daucus Carota L.) and Carrot Puree. *J. Agric. Food Chem.* **2003**, *51* (13), 3865–3873. https://doi.org/10.1021/jf034085+.

(5) Scharbert, S.; Holzmann, N.; Hofmann, T. Identification of the Astringent Taste Compounds in Black Tea Infusions by Combining Instrumental Analysis and Human Bioresponse. *J. Agric. Food Chem.* **2004**, *52* (11), 3498–3508. https://doi.org/10.1021/jf049802u.

(6) Scharbert, S. T. H. Molecular Definition of Black Tea Taste by Means of Quantitative Studies , Taste Reconstitution , and Omission Experiments. *J. Agric. Food Chem.* **2005**, *53*, 5377–5384.

(7) Hagerman, A. E.; Butler, L. G. Protein Precipitation Method for the Quantitative Determination of Tannins. *J. Agric. Food Chem.* **1978**, *26* (4), 809–812. https://doi.org/10.1021/jf60218a027.

(8) Sousa, A. D.; Maia, I. V.; Ribeiro, P. R. V.; Canuto, K. M.; Zocolo, G. J.; Sousa de Brito, E. UPLC-QTOF-MSE-Based Chemometric Approach Driving the Choice of the Best Extraction Process for Phyllanthus Niruri. *Sep. Sci. Technol.* **2017**, *52* (10), 1696–1706. https://doi.org/10.1080/01496395.2017.1298612.

(9) Oiram Filho, F.; Zocolo, G. J.; Canuto, K. M.; Silva Junior, I. J. da; Brito, E. S. Productivity of a Preparative High-performance Liquid Chromatography Isolation of Anacardic Acids from Cashew Nut Shell Liquid. *Sep. Sci. Plus* **2019**,

2 (6), 192–199. https://doi.org/10.1002/sscp.201900014.

(10) Oiram Filho, F.; Alcântra, D. B.; Rodrigues, T. H. S.; Alexandre Silva, L. M.; De Oliveira Silva, E.; Zocolo, G. J.; De Brito, E. S. Development and Validation of a Reversed Phase HPLC Method for Determination of Anacardic Acids in Cashew (Anacardium Occidentale) Nut Shell Liquid. *J. Chromatogr. Sci.* **2018**, *56* (4), 300–306. https://doi.org/10.1093/chromsci/bmx111.

(11) Fang, Y. T.; Li, Q.; Cao, A. C.; Li, Y.; Wei, Y. Isolation and Purification of Phenolic Acids from Sugarcane (Saccharum Officinarum L.) Rinds by PH-Zone-Refining Counter-Current Chromatography and Their Antioxidant Activity Evaluation. *Food Anal. Methods* **2017**, *10* (7), 2576–2584. https://doi.org/10.1007/s12161-017-0824-3.

(12) Das, I.; Arora, A. Post-Harvest Processing Technology for Cashew Apple – A Review. *J. Food Eng.* **2017**, *194*, 87–98. https://doi.org/10.1016/j.jfoodeng.2016.09.011.

(13) Halgren, T. A. Merck Molecular Force Field. *J. Comput. Chem.* **1996**, *17*, 490–519.

(14) Gandhi, A. K.; Kim, W. M.; Sun, Z. J.; Huang, Y.; Bonsor, D. A.; Sundberg, E. J.; Kondo, Y.; Wagner, G.; Kuchroo, V. K.; Petsko, G.; Blumberg, R. S. High Resolution X-Ray and NMR Structural Study of Human T-Cell Immunoglobulin and Mucin Domain Containing Protein-3. *Sci. Rep.* **2018**, No. July, 1–13. https://doi.org/10.1038/s41598-018-35754-0.

(15) Vanommeslaeghe, K.; Hatcher, E.; Acharya, C.; Kundu, S.; Zhong, S.; Shim, J.; Darian, E. CHARMM General Force Field : A Force Field for Drug-Like Molecules Compatible with the CHARMM All-Atom Additive Biological Force

Fields. *Wiley Intersci.* **2009**, *31*. https://doi.org/10.1002/jcc.

(16) Spoel, D. V. A. N. D. E. R.; Lindahl, E.; Hess, B.; Groenhof, G. GROMACS: Fast, Flexible, and Free. *Wiley Intersci.* **2005**, *26*. https://doi.org/10.1002/jcc.20291.

(17) Vanommeslaeghe, K.; Mackerell, A. D. Automation of the CHARMM General Force Field (CGenFF) I: Bond Perception and Atom Typing. *J. Chem. Inf. Model.* **2012**, *52* (1), 3144–3154. https://doi.org/10.1021/ci300363c.

(18) Vanommeslaeghe, K.; Raman, E. P.; Mackerell, A. D. Automation of the CHARMM General Force Field (CGenFF) II: Assignment of Bonded Parameters and Partial Atomic Charges. *J. Chem. Inf. Model.* **2012**, *52*, 3155–3169. https://doi.org/10.1021/ci3003649.

(19) Yu, W.; He, X.; Vanommeslaeghe, K.; Mackerell, A. D. Extension of the CHARMM General Force Field to Sulfonyl-Containing Compounds and Its Utility in Biomolecular Simulations. *J. Comput. Chem.* **2012**, *33*, 2451–2468. https://doi.org/10.1002/jcc.23067.

(20) Soteras, I.; Lin, F.; Vanommeslaeghe, K.; Lemkul, J. A.; Armacost, K. A.; Brooks, C. L.; Mackerell, A. D. Parametrization of Halogen Bonds in the CHARMM General Force Field : Improved Treatment of Ligand – Protein Interactions. *Biooganica Med. Chem.* **2016**, *24*, 4812–4825. https://doi.org/10.1016/j.bmc.2016.06.034.

(21) Bussi, G.; Donadio, D.; Parrinello, M.; Bussi, G.; Donadio, D.; Parrinello, M. Canonical Sampling through Velocity Rescaling Canonical Sampling through Velocity Rescaling. *J. Chem. Phys.* **2007**, *014101*. https://doi.org/10.1063/1.2408420.

(22) Berendsen, H. J. C.; Postma, J. P. M.; van Gunsteren, W. F.; DiNola, A.; Haak, J. R. Molecular Dynamics with Coupling to an External Bath. *J. Chem. Phys.* **1984**, *3684* (April 1984), 3684–3690. https://doi.org/https://doi.org/10.1063/1.448118.

(23) Seong, Y. A.; Shin, P. G.; Yoon, J. S.; Yadunandam, A. K.; Kim, G. Do. Induction of the Endoplasmic Reticulum Stress and Autophagy in Human Lung Carcinoma A549 Cells by Anacardic Acid. *Cell Biochem. Biophys.* **2014**, *68* (2), 369–377. https://doi.org/10.1007/s12013-013-9717-2.

(24) Agostini-Costa, T. da S.; Jales, K. A.; Garruti, D. dos S.; Padilha, V. A.; Lima, J. B. De; Aguiar, M. D. J.; de Paiva, J. R. Teores de Ácido Anacárdico Em Pedúnculos de Cajueiro Anacardium Microcarpum e Em Oito Clones de Anacardium Occidentale Var . Nanum Disponíveis No Nordeste Do Brasil. *Ciência Rural* **2004**, *34*.

(25) Golebiowski, J.; Fiorucci, Ś.; Adrian-Scotto, M.; Fernandez-Carmona, J.; Antonczak, S. Molecular Features Underlying the Perception of Astringency as Probed by Molecular Modeling. *Mol. Inform.* **2011**, *30* (5), 410–414. https://doi.org/10.1002/minf.201000165.

(26) Cala, O.; Dufourc, E. J.; Fouquet, E.; Manigand, C.; Laguerre, M.; Pianet, I. The Colloidal State of Tannins Impacts the Nature of Their Interaction with Proteins: The Case of Salivary Proline-Rich Protein/Procyanidins Binding. *Langmuir* **2012**, *28* (50), 17410–17418. https://doi.org/10.1021/la303964m.

(27) Omanakuttan, A.; Nambiar, J.; Harris, R. M.; Bose, C.; Pandurangan, N.; Varghese, R. K.; Kumar, G. B.; Tainer, J. A.; Banerji, A.; Perry, J. J. P.; Nair, B. G. Anacardic Acid Inhibits the Catalytic Activity of Matrix Metalloproteinase-2 and Matrix Metalloproteinase-9. *Mol. Pharmacol.* **2012**, *82* (4), 614–622.

https://doi.org/10.1124/mol.112.079020.

(28) Sacconnay, L.; Angleviel, M.; Randazzo, G. M.; Marçal Ferreira Queiroz, M.; Ferreira Queiroz, E.; Wolfender, J. L.; Carrupt, P. A.; Nurisso, A. Computational Studies on Sirtuins from Trypanosoma Cruzi: Structures, Conformations and Interactions with Phytochemicals. *PLoS Negl. Trop. Dis.* **2014**, *8* (2). https://doi.org/10.1371/journal.pntd.0002689.

(29) Schultz, D. J.; Wickramasinghe, N. S.; Ivanova, M. M.; Isaacs, S. M.; Dougherty, S. M.; Imbert-Fernandez, Y.; Cunningham, A. R.; Chen, C.; Klinge, C. M. Anacardic Acid Inhibits Estrogen Receptor α-DNA Binding and Reduces Target Gene Transcription and Breast Cancer Cell Proliferation. *Mol. Cancer Ther.* **2010**, *9* (3), 594–605. https://doi.org/10.1158/1535-7163.MCT-09-0978.

(30) Wu, Y.; He, L.; Zhang, L.; Chen, J.; Yi, Z.; Zhang, J.; Liu, M.; Pang, X. Anacardic Acid (6-Pentadecylsalicylic Acid) Inhibits Tumor Angiogenesis by Targeting Src/FAK/Rho GTpases Signaling Pathway. *J. Pharmacol. Exp. Ther.* **2011**, *339* (2), 403–411. https://doi.org/10.1124/jpet.111.181891.

(31) Ryckewaert, L.; Sacconnay, L.; Carrupt, P. A.; Nurisso, A.; Simões-Pires, C. Non-Specific SIRT Inhibition as a Mechanism for the Cytotoxicity of Ginkgolic Acids and Urushiols. *Toxicol. Lett.* **2014**, *229* (2), 374–380. https://doi.org/10.1016/j.toxlet.2014.07.002.

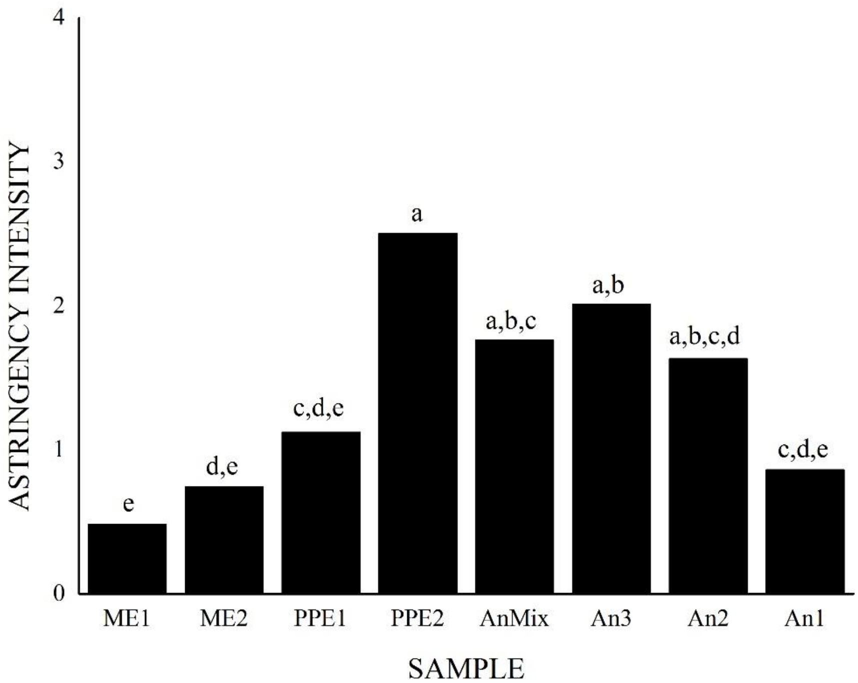

Fig. 1. Sensory mean for astringency intensity for cashew apple extracts.

Footnote: ME1= Methanolic cashew extract (2 $mg.mL^{-1}$); ME2= Methanolic cashew extract (5 $mg.mL^{-1}$); PPE1= Cashew protein precipitate extract (1 $mg.mL^{-1}$); PPE2= Cashew protein precipitate extract (2 $mg.mL^{-1}$); AnMix= Anacardic acid mixture(1 $mg.mL^{-1}$); An3= Anacardic acid 15:3 (1 $mg.mL^{-1}$); An2= Anacardic acid 15:2 (1 $mg.mL^{-1}$); An1= Anacardic acid 15:1 (1 $mg.mL^{-1}$). Astringency scale ranging from 0 to 4, being: 0 = not astringent and 4 = extremely astringent.

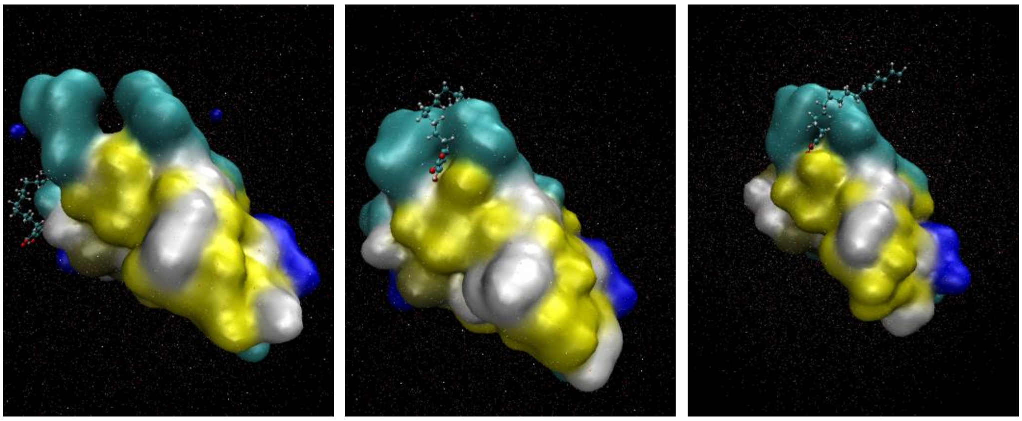

Fig. 2. Rendered structures of the final conformation at 10 ns for anacardic acids (a) monoene, (b) diene, and (c) triene.

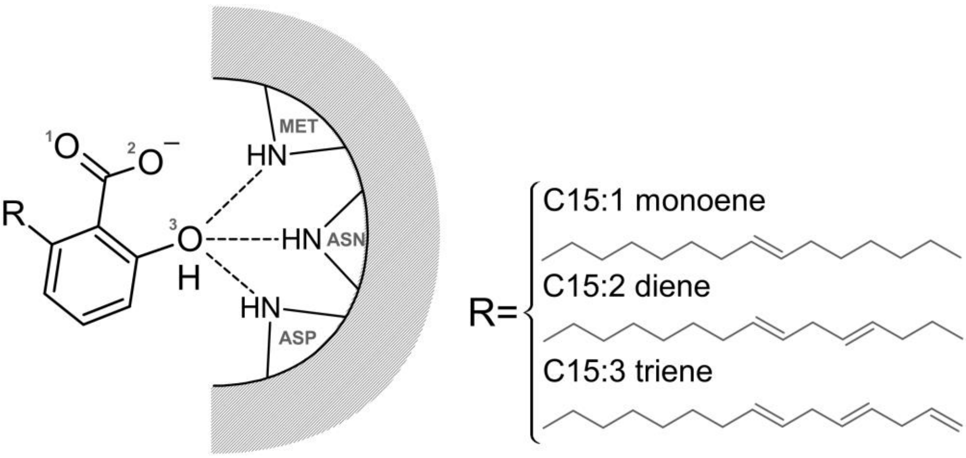

Fig. 3. Schematic representation of the hydrogen bond established between 6DHB and the carboxyl and hydroxyl groups of anacardic acids.

Table 1

Identification by UPLC-QTOF-MS^E of the compounds presents in the methanolic extract, protein non-complexed fraction; and cashew protein precipitate extract.

t_R min	$[M\text{-}H]^-$ Observed	$[M\text{-}H]^-$ Calculated	Product Ions (MS/MS)	Empirical Formula	Error (Ppm)	Putative Name	Methanolic Extract	Supernatant	Protein Precipitate	References
4.31	939.1116	939.1104	617.0893; 769.0878	$C_{41}H_{32}O_{26}$	4.7	Pentagaloyl Hexoside	✓	✓	✓	Abu-Reidah et al., 2015
8.00	397.1325	397.1346	-	$C_{15}H_{26}O_{12}$	-5.3	N.I	✓		✓	
9.03	531.3145	531.3169	-	$C_{27}H_{48}O_{10}$	-4.5	N.I	✓		✓	
9.81	341.2104	341.2117	297.2203; 119.0496	$C_{22}H_{30}O_3$	-3.8	Anacardic Acid (15:3)	✓	✓	✓	Cunha et al., 2017
10.56	343.2245	343.2273	299.2225; 106.0394	$C_{22}H_{32}O_3$	-2.8	Anacardic Acid (15:2)	✓	✓	✓	Cunha et al., 2017
11.47	345.2412	345.2430	301.2463; 106.0413	$C_{22}H_{34}O_3$	-5.2	Anacardic Acid (15:1)	✓	✓	✓	Oiram Filho et al., 2017
12.76	373.2734	373.2743	329.2870; 106.0439	$C_{24}H_{38}O_3$	-2.4	Anacardic Acid (17:1)	✓		✓	Oiram Filho et al., 2017

Table 2.

Decomposition of the short-range energies for the protein-ligand complex between the mucin 6DHB and the mono, di and triene anacardic acid derivatives.

Average short-range Coulombic interaction energy (protein-ligand)				
Mol	Energy	Average	RMSD	Tot-Drift /(kJ mol^{-1})
monoene	Coul-SR:Protein-Monoene	-55.7639±24	62.7515	152.689
diene	Coul-SR:Protein-Diene	-68.748±13	54.0877	99.7627
triene	Coul-SR:Protein-Triene	-76.9496±6.4	54.8268	-3.29316
Average short-range Lennard-Jones interaction energy (protein-ligand)				
Mol	Energy	Average	RMSD	Tot-Drift /(kJ/mol)
monoene	LJ-SR:Protein-Monoene	-61.5651±7.8	25.2576	39.1442
diene	LJ-SR:Protein-Diene	-77.7686±1.9	12.062	6.17392
triene	LJ-SR:Protein-Triene	-78.4396±5.6	19.0896	-0.0896526

Table 3.

Hydrogen bond (HB) distances between each oxygen (HB acceptor) from the anacardic acids (monoene C15:1, diene C15:2, and triene C15:3) and the nitrogen (HB donor) of the amino group of each of the three main aminoacids (MET: methionine, ASN: asparagines, ASP: aspartate) of the active site of 6DHB.

		(N)MET	(N)ASN	(N)ASP
	O1	0.770±0.081	0.631±0.086	0.669±0.083
C15:3	O2	0.695±0.079	0.497±0.081	0.485±0.094
	O3	0.546±0.068	0.368±0.053	0.333±0.054
	O1	0.796±0.088	0.665±0.090	0.699±0.077
C15:2	O2	0.724±0.087	0.529±0.094	0.516±0.095
	O3	0.572±0.077	0.382±0.071	0.338±0.065
	O1	0.983±0.456	0.988±0.430	1.050±0.432
C15:1	O2	0.961±0.530	0.932±0.529	0.972±0.550
	O3	0.873±0.601	0.838±0.606	0.859±0.638

520 **Graphical abstract**

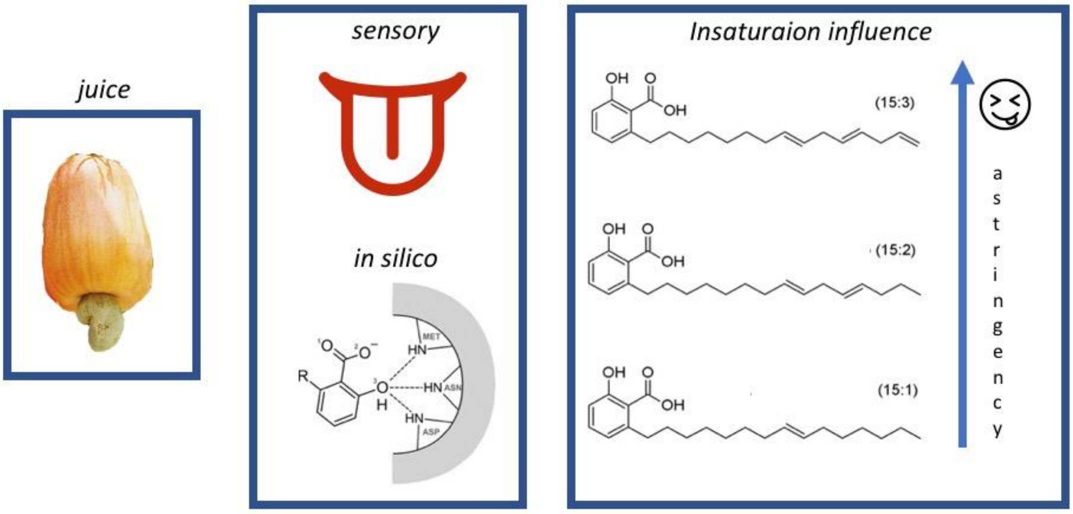

521